Linked and Fused Tungstaborane Clusters: Synthesis, Characterization, and Electronic Structures of *bis*-{(η^5-$C_5Me_5W)_2B_5H_8$}$_2$ and (η^5-$C_5Me_5W)_2${$Fe(CO)_3$}$_nB_{6-n}H_{10-n}$, $n = 0, 1$†

Shubhankar Kumar Bose and Sundargopal Ghosh*

Department of Chemistry, Indian Institute of Technology, Madras, Chennai 600 036, India

Bruce C. Noll

Department of Chemistry and Biochemistry, University of Notre Dame, Notre Dame, Indiana 46556

Jean-Francois Halet and Jean-Yves Saillard

Sciences Chimiques de Rennes, UMR 6226 CNRS-Université de Rennes 1, Avenue du Général Leclerc, 35042 Rennes Cedex, France

Andrés Vega

Departamento de Quimica, Facultad de Ecología y Recursos Naturales, Universidad Nacional Andres Bello Republica 275, Santiago, Chile

Received June 9, 2007

In addition to (η^5-$C_5Me_5W)_2B_5H_9$, (η^5-$C_5Me_5W)_3(\mu$-H)B_8H_8, and (η^5-$C_5Me_5W)_2B_7H_9$ reported earlier, thermolysis of {η^5-C_5Me_5W}$H_3B_4H_8$ (**1**) with BH_3·THF leads to the formation of bicapped *closo*-{η^5-C_5Me_5W}$_2B_6H_{10}$ (**2**) in parallel with a B−B linked dimer of {η^5-C_5Me_5W}$_2B_5H_9$ (**4**) and bis-{(η^5-$C_5Me_5W)_2B_5H_8$}$_2$ (**3**). Reaction of **4** with a 3-fold excess of $Fe_2(CO)_9$ in hexane generates an iron analogue of **2**, (η^5-$C_5Me_5W)_2B_5H_9Fe(CO)_3$ (**5**) in 46% yield. All the metallaboranes, **2**, **3**, and **5**, have been characterized by ^{1}H, ^{11}B NMR spectra and crystal structure determinations. The structures of **2** and **5** appear to follow the regular electron counting rules as they possess seven skeletal electron pairs (sep) appropriate for bicapped octahedral structures. However, their electronic structures revealed by a molecular orbital analysis is more closely related to that of [{η^5-C_5Me_5Re}$_2B_7H_7$], a cluster that does not obey the classical electron counting rules. Clusters **2** and **5** are notable examples of closo clusters containing four bridging hydrogens. **3** is a coupled-cage structure in which two bicapped trigonal bipyramidal frameworks, W_2B_5, are joined by an exopolyhedral boron−boron bond.

Introduction

In metallacarborane chemistry, three complementary approaches to the expansion of cluster networks containing transition metal fragments have received much attention:[1,2] (i) condensation involving monoborane reagents, (ii) insertion or fragmentation involving borane or metal carbonyl fragments, and (iii) intercluster fusion with two or more atoms held in common between the constituent subclusters. In each case, reaction often leads to the formation of a range of products with varying M:B ratios and, as shown in this work, all three modes can lead to products competitively in a single system.

After discovering that the reaction of (η^5-$C_5Me_5M)_2B_4H_8$, M = Re and Ru, with borane led to the isolation of hypoelectronic rhenaboranes, (η^5-$C_5Me_5Re)_2B_nH_n$, $n = 7-10$,[3] hydrogen-rich, ruthenaboranes, (η^5-$C_5Me_5Ru)_2B_nH_{12}$, $n = 6$, 8,[4] and (η^5-$C_5Me_5Ru)_2B_{10}H_{16}$[5] a reinvestigation of a related tungsten system became attractive. Earlier, the thermolysis of hydrogen-rich {η^5-$C_5Me_5WH_3$}B_4H_8 (**1**) at 110 °C produced 7-atom (η^5-$C_5Me_5W)_2B_5H_9$, 11-atom (η^5-$C_5Me_5W)_3(\mu$-H)B_8H_8, and 9-atom (η^5-$C_5Me_5W)_2B_7H_9$ clusters.[6] As the rhenium work suggested that higher nuclearity clusters than previously thought might now be accessible and the (η^5-$C_5Me_5W)_2B_7H_9$ cluster is isoelectronic with (η^5-$C_5Me_5Re)_2B_7H_7$, the tungsten system was reinvestigated. As a result, a coupled metallaborane with a total of 14-cluster atoms, *bis*-{(η^5-$C_5Me_5W)_2B_5H_8$}$_2$ (**3**), and a capped cluster with 8 atoms, {η^5-C_5Me_5W}$_2B_6H_{10}$ (**2**), were isolated. Although the later is no larger than any of the earlier products, it provides a link between the electronic structures of (η^5-$C_5Me_5W)_2B_7H_9$ and (η^5-$C_5Me_5Re)_2B_7H_7$.[6] The seven-sep bicapped

† Dedicated to Professor Thomas P. Fehlner on the occasion of his 70th birthday.

* To whom correspondence should be addressed. E-mail: sghosh@iitm.ac.in.

(1) (a) Kennedy, J. D. *Prog. Inorg. Chem.* **1984**, *32*, 519. (b) Kennedy, J. D. *Prog. Inorg. Chem.* **1986**, *34*, 211.

(2) Wang, X.; Sabat, M.; Grimes, R. N. *Organometallics* **1995**, *14*, 4668.

(3) Le Guennic, B.; Jiao, H.; Kahlal, S.; Saillard, J.-Y.; Halet, J.-F.; Ghosh, S.; Beatty, A. M.; Rheingold, A. L.; Fehlner, T. P. *J. Am. Chem. Soc.* **2004**, *126*, 3203.

(4) Ghosh, S.; Beatty, A. M.; Fehlner, T. P. *Angew. Chem., Int. Ed.* **2003**, *42*, 4678.

(5) Ghosh, S.; Noll, B. C.; Fehlner, T. P. *Angew. Chem., Int. Ed.* **2005**, *44*, 2916.

(6) Weller, A. S.; Shang, M.; Fehlner, T. P. *Organometallics* **1999**, *18*, 853.

10.1021/om700565f CCC: $37.00
Publication on Web 09/27/2007

Scheme 1

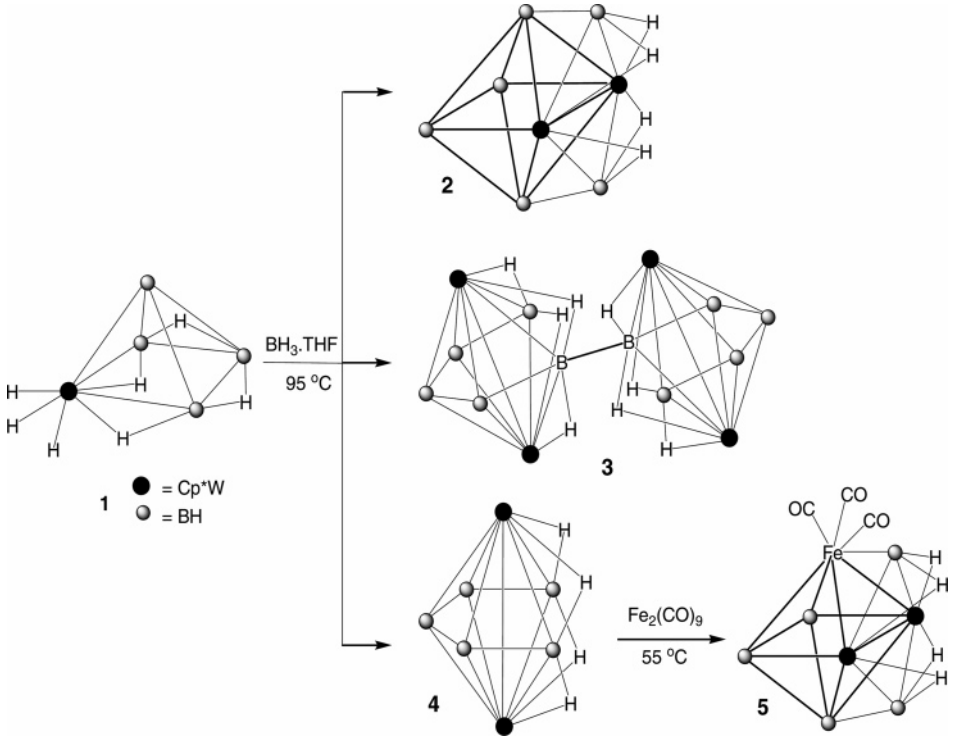

octahedral architecture of **2** satisfies the electron counting rules derived from the borane analogy; however, there is a striking relationship between $(\eta^5\text{-}C_5Me_5Re)_2B_7H_7$ and **2**. For this reason theoretical calculations using the density functional theory (DFT) methods were carried out on a simplified model of **2**, $(CpW)_2B_6H_{10}$ (**2′**), to probe the nature of the relationship of the actual electronic structures. As will be seen, surprisingly **2** can also be described as an electron deficient metalloborane with a cluster architecture derived from that of $(\eta^5\text{-}C_5Me_5Re)_2B_6H_4Cl_2$.[7]

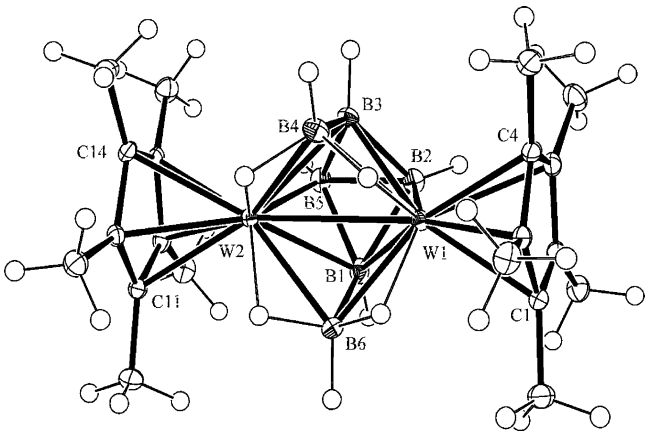

Figure 1. Molecular structure of $(\eta^5\text{-}C_5Me_5W)_2B_6H_{10}$ (**2**). Bond distances (Å) and angles (deg): W(1)−W(2), 2.95850(12); W(1)−B(1), 2.354(2); W(1)−B(3), 2.349(3); W(1)−B(2), 2.155(3); W(1)−B(6), 2.294(3); W(1)−B(4), 2.283(3); B(1)−B(5), 1.777(4); B(1)−B(6), 1.820(4); B(2)−B(5), 1.697(4); B(3)−B(4), 1.820(4); B(2)−W(1)−B(6), 92.14(10); B(6)−W(1)−B(3), 97.62(9); B(2)−W(1)−B(3), 46.63(10); B(3)−W(1)−B(1), 69.37(9); B(2)−W(1)−W(2), 72.95(7); B(1)−W(1)−W(2), 50.72(6); C(2)−W(1)−W(2), 149.37(5).

Results and Discussion

Reaction of $[\{(\eta^5\text{-}C_5Me_5)WH_3\}B_4H_8]$ with BH_3·THF. Thermolysis of $[\{(\eta^5\text{-}C_5Me_5)WH_3\}B_4H_8]$[8] (**1**) with BH_3·THF at 95 °C for 20 h yields metallaboranes $\{(\eta^5\text{-}C_5Me_5W)_2B_6H_{10}\}$ (**2**) and $\{(\eta^5\text{-}C_5Me_5W)_2B_5H_8\}_2$ (**3**) in yields of 12 and 5% (Scheme 1). In parallel with **2** and **3**, $\{(\eta^5\text{-}C_5Me_5W)_2B_5H_9\}$ (**4**), $\{(\eta^5\text{-}C_5Me_5W)_3(\mu\text{-}H)B_8H_8\}$, and $(\eta^5\text{-}C_5Me_5W)_2B_7H_9$ are also formed as reported previously.[6] The composition and structure of **2** is established from the mass spectral analysis, NMR, and X-ray diffraction studies. The exact mass measurement of **2** gives a molecular ion corresponding to $C_{20}H_{40}B_6W_2$. The ^{11}B NMR spectrum shows three types of boron environments in the ratio of 1:1:1. The $^1H\{^{11}B\}$ NMR spectrum reveals three types of B−H protons in the ratio of 1:1:1 and the presence of one high-field ^1H resonance at δ −15.79 ppm of intensity 4. The NMR data of **2** suggest a plane of symmetry for a static molecule as well as the presence of one type of W−H−B bridging proton.

The NMR data on **2** are consistent with the solid-state X-ray structure of *closo*-2,3-$(\eta^5\text{-}C_5Me_5W)_2B_6H_{10}$, shown in Figure 1. The observed bicapped octahedral closo-cluster geometry is well known, even though closo clusters with four edge-bridging WHB hydrogens are rare. Other examples are $(\eta^5\text{-}C_5Me_5W)_2B_5H_9\text{-}Fe(CO)_3$ (vide infra) and $(\eta^5\text{-}C_5Me_5Mo)_2B_5H_9Fe(CO)_3$[9], generated from $(\eta^5\text{-}C_5Me_5Mo)_2B_5H_9$.[10] A $^1H\{^{11}B\}$ selective NMR experiment of **2** shows that the four W−H protons are coupled exclusively to the capping boron atoms. The bicapped octahedral geometry of **2** can be compared with that of *closo*-$(\eta^5\text{-}C_5Me_5\text{-}Ru)_2B_6H_3Cl_3$[11] (Scheme 2, vide infra).

(7) Ghosh, S.; Beatty, A. M.; Fehlner, T. P. *J. Am. Chem. Soc.* **2001**, *123*, 9188.
(8) Weller, A. S.; Shang, M.; Fehlner, T. P. *Organometallics* **1999**, *18*, 53.
(9) Aldridge, S.; Hashimoto, H.; Kawamura, K.; Shang, M.; Fehlner, T. P. *Inorg. Chem.* **1998**, *37*, 928.
(10) Kim, D. Y.; Girolami, G. S. *J. Am. Chem. Soc.* **2006**, *128*, 10969.

Scheme 2. Formation of mono- and bicapped Ruthenaboranes from *nido*-1,2-(η^5- $C_5Me_5Ru)_2(\mu$-H)$_2B_3H_7$ (B-*H*-B Hydrogens Are Not Shown for Clarity)

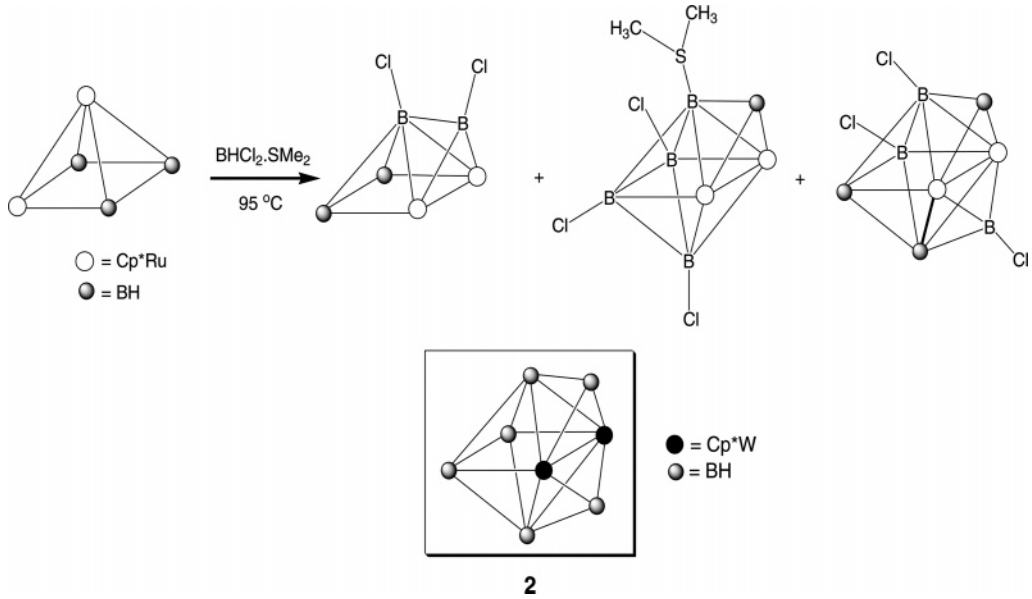

2

The second new metallaborane product, **3**, has been isolated following thin layer chromatography (TLC) in air in low yield and was characterized spectroscopically and with X-ray diffraction studies. The molecular structure revealed that compound **3** is a dimer of (η^5-$C_5Me_5W)_2B_5H_9$ joined by means of an exopolyhedral boron−boron bond (Figure 2), and it has a crystallographically generated C_2 axis making each cluster cage unit equivalent . Two bicapped trigonal bipyramidal cages are joined by means of an exopolyhedral boron−boron bond in the B5 position (capping boron atom of the bicapped trigonal bipyramid). The intercluster B−B distance (1.75(2) Å) in **3** is similar to an unbridged B−B distance in the cluster B(5)−B(4) (1.740(16) Å) and therefore, longer than normally observed in other boron−boron coupled species, for example, 5,5′-{η^5-$C_5Me_5Co(Et_2C_2B_4H_3)\}_2$[2] (1.690(6) Å), 1,2′-$(B_5H_8)_2$[12] (1.660(8) Å), and $C_2B_8H_{11}$−$C_2B_{10}H_{11}$[13] (1.681(2) Å). The average intracluster distances in **3** are similar to those observed in the monomer[6,14] ($d_{W-W} = 2.81$, $d_{W-B} = 2.22$, and $d_{B-B} = 1.71$ Å). As expected the formation of the exopolyhedral boron−boron linkage does not perturb the cluster bonding pattern significantly.

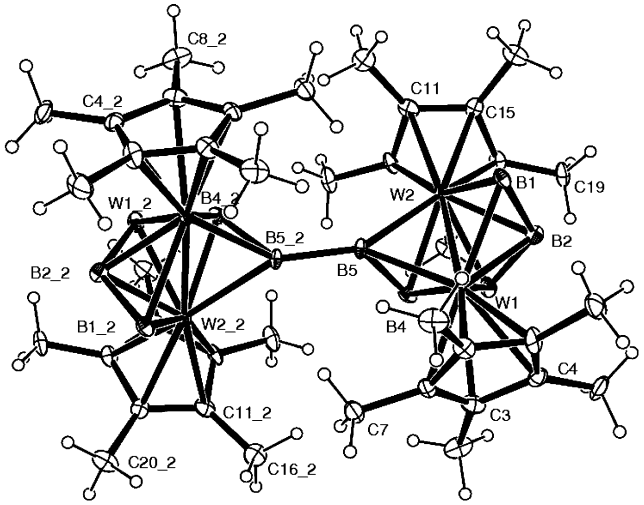

Figure 2. Molecular structure of *bis*-{(η^5-$C_5Me_5W)_2B_5H_8\}_2$ (**3**). Bond distances (Å) and angles (deg): W(1)−W(2), 2.8167(6); W(1_2)−W(2_2), 2.826(12); B(5)−B(5_2), 1.75(2); B(1)−B(2), 1.767(16); B(3)−B(4), 1.705(16); B(2)−B(3), 1.699(16); B(4)−B(5), 1.740(16); W(1)−B(5), 2.333(11); W(1)−B(3), 2.208(11); B(1)−W(1)−B(5), 89.2(4); B(3)−W(1)−B(4), 45.3(4); B(1)−W(1)−W(2), 52.6(3); B(4_2)−W(1_2)−B(2_2), 87.5(5); W(1)−B(5)−W(2), 74.2(3); B(5_2)−B(5)−W(2), 146.8(7); B(4)−B(5)−B(5_2), 124.6(8).

The spectroscopic data for **3** in solution also support the solid-state structure. The mass spectrum in the high *m*/*z* range shows a molecular ion peak at *m*/*z* 1399 corroborating the crystallographic composition. Compound **3** has five different B-environments; however, the ^{11}B NMR spectrum shows four resonances in the intensity ratio of 2:1:1:1 where integral 2 resonance is due to the 1+1 coincidence. This formulation of compound **3** rationalizes the presence two kinds of Cp* and four kinds of WHB protons in the ^{1}H NMR. The broad resonance at δ 40.6 ppm of intensity two is assigned to the boron atoms linked by a single bond, and its breadth makes a definitive conclusion concerning the absence of BH coupling.

Although there are exceptions,[15] borane, heteroborane, and metallaborane chemistry is largely governed at present by single polyhedral clusters with a natural size limit of 12 vertices. However, cluster fusion is an alternative yielding significant new cluster systems.[16] Thus clusters linked or fused together in a covalent manner constitute one way to bigger cluster assemblies. The simplest way of linking two clusters together is by a two-electron, two center, B−B σ bond.[16,17] Some known examples are the isomers of bis(*nido*-decaboranyl), {$(B_{10}H_{13})_2$}[18] and {$B_{20}H_{28}$},[19] which have a central *nido*-{$B_{10}H_{12}$} core with

(11) Ghosh, S.; Fehlner, T. P.; Beatty, A. M.; Noll, B. C. *Organometallics* **2005**, *24*, 2473.
(12) Briguglio, J. J.; Carroll, P. J.; Corcoran, E. W.; Sneddon, L. G. *Inorg. Chem.* **1986**, *25*, 4618.
(13) Subrtova, V.; Linek, A.; Hasek, J. *Acta Cryst.* **1982**, *B38*, 3147.
(14) Bullick, H. J.; Grenbenik, P. D.; Green, M. L. H.; Hughes, A. K.; Leach, J. B.; McGowan, P. C. *J. Chem. Soc., Dalton Trans.* **1995**, 67.
(15) (a) Burke, A.; Ellis, D.; Giles, B. T.; Hodson, B. E.; Macgregor, S. A.; Rosiar, G. M.; Welch, A. J. *Angew. Chem., Int. Ed.* **2003**, *42*, 225. (b) Deng, L.; Chan, H.-S.; Xie, Z. *Angew. Chem., Int. Ed.* **2005**, *44*, 2128. (c) Deng, L.; Zhang, J.; Chan, H.-S.; Xie, Z. *Angew. Chem., Int. Ed.* **2006**, *45*, 4309. (d) McIntosh, R. D.; Ellis, D.; Rosiar, G. M.; Welch, A. J. *Angew. Chem., Int. Ed.* **2006**, *45*, 4313. (e) Deng, L.; Xie, Z. *Organometallics* **2007**, *26*, 1832 and references therein.

Chart 1. B−B Linked Clusters

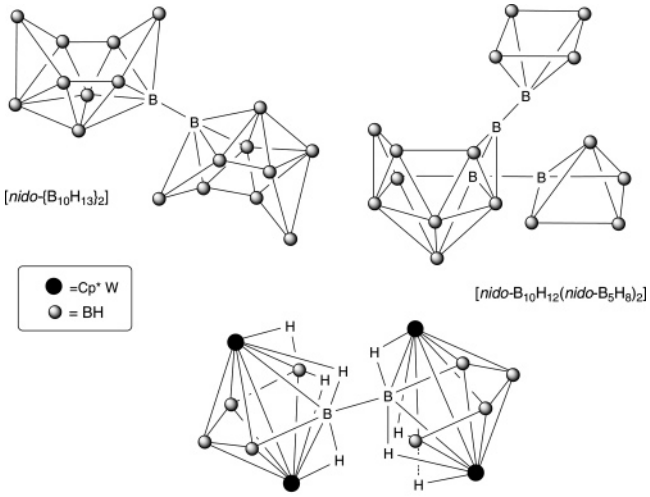

3

two *nido*{B_5H_8} units bound to them at mutually adjacent positions (Chart 1).

A second method of bypassing single clusters size limit is by capping. Although not known for pure *p*-block clusters, the structural motif is well represented in metal cluster chemistry.[20] It is also well represented in metallaborane chemistry.[21] For example, reaction of *nido*-1,2-(η^5-$C_5Me_5Ru)_2(\mu$-H)$_2B_3H_7$ with $BHCl_2{\cdot}SMe_2$ in toluene at 95 °C leads to the formation of three different types of capped metallaboranes:[11] monocapped square pyramidal, *pileo*-2,3-(η^5-$C_5Me_5Ru)_2(\mu$-H)$B_4H_5Cl_2$, monocapped octahedral, *closo*-1-(SMe_2)-2,3-(η^5-$C_5Me_5Ru)_2(\mu_3$-H)B_5HCl_3, and bicapped octahedral, *closo*-2,3-(η^5-$C_5Me_5Ru)_2B_6H_3Cl_3$ (Scheme 2).

Reaction of (η^5-$C_5Me_5W)_2B_5H_9$ with $Fe_2(CO)_9$. Reaction of **4** with 3-fold excess of $Fe_2(CO)_9$ in hexane generates a single metallaborane product in yields of 46% based on the amount of $(Cp^*W)_2B_5H_9$ (**4**) taken. Mass spectral analysis is consistent with a compound of the formulation (η^5-$C_5Me_5W)_2B_5H_9Fe(CO)_3$ formed by addition of a single $Fe(CO)_3$ fragment to **4**. Four signals are observed in the ^{11}B NMR spectrum at δ 84.2, 46.2, 39.1, and −6.6 ppm (2:1:1:1), together with a single Cp* resonance at δ 1.88 ppm, two bridging hydrogen signals at δ −15.33 and δ −16.92 ppm (2:2), and three terminal BH signals at δ 8.65, 6.51, and 4.41 ppm in the ^{1}H NMR spectrum.

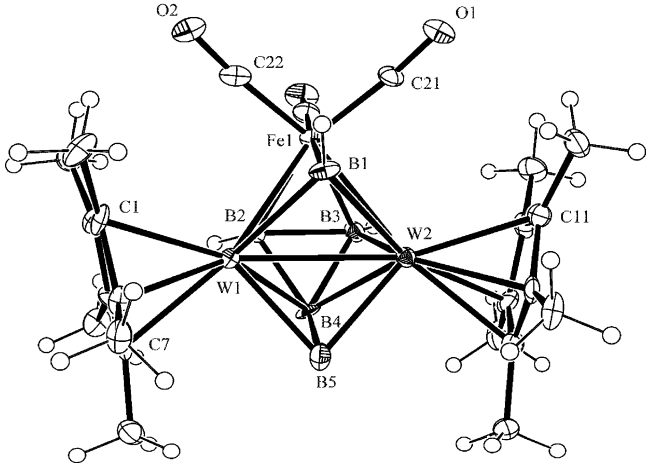

Figure 3. Molecular structure of [(η^5-$C_5Me_5W)_2B_5H_9Fe(CO)_3$] (**5**). Bond distances (Å) and angles (deg): W(1)−W(2), 2.9392(7); Fe(1)−B(2), 2.182(15); Fe(1)−W(2), 2.760(2); W(1)−B(2), 2.172(18); W(1)−B(5), 2.261(17); W(1)−B(1), 2.351(17); W(2)−B(4), 2.344(17); B(2)−B(4), 1.75(2); B(4)−B(5), 1.83(3); B(1)−Fe(1)−B(2), 103.8(6); B(3)−Fe(1)−B(2), 47.8(6); B(2)−W(1)−B(5), 92.4(6); W(1)−Fe(1)−W(2), 64.35(5); B(2)−Fe(1)−W(1), 50.5(5); B(4)−W(1)−B(1), 100.6(6); W(1)−B(1)−W(2), 77.1(4); Fe(1)−B(1)−W(2), 74.9(5).

The molecular structure of **5** in the solid state, shown in Figure 3, is a bicapped octahedron, with W(1), W(2), B(2), B(3), B(4), and Fe(1) occupying the vertices of the core octahedron, capped by two BH groups. Although the crystal structure of **5** does not display the W−H−B hydrogens, the position of the bridging W−H−B hydrides are assigned by comparing with those of the ^{1}H{^{11}B} resonances of δ −15.79 (W−H−B) in **2** and −6.78 ppm (Fe−H−B) in $Fe_2(CO)_6$(η^5-C_5Me_5RuCO)(η^5-$C_5Me_5Ru)B_6H_{10}$.[22] Addition of the two-electron three-orbital $Fe(CO)_3$ fragment, into a six-sep bicapped trigonal bypyramid as observed in **4**, changes the geometry to bicapped octahedral in keeping with the changes predicted by the Wade/Mingos rule.[23]

The $Fe(CO)_3$ fragment is isolobal with the BH group and a replacement of one BH fragment by a $Fe(CO)_3$ unit from (η^5-$C_5Me_5W)_2B_6H_{10}$ would generate (η^5-$C_5Me_5W)_2B_5H_9Fe(CO)_3$ (**5**). Thus, the qualitative cluster shapes of **2** and **5** are the same, and differences are sought in the magnitude of the structural parameters and positioning of the capping atoms. The W−W bond distances of **2** and **5** (2.95850(12) Å in **2** and 2.9392(7) Å in **5**) are somewhat longer than that found in **4** (2.8170(8) Å). The W−B (capping boron) distances (viz. W−B(6) and W−B(4)) in **2** are almost similar however, they are different in **5** (e.g., W2−B1, 2.363(15) Å and W2−B5, 2.254(18) Å). This might be due to the presence of one $Fe(CO)_3$ unit in the octahedral core of **5**.

In the area of metallaboranes, a number of closo-cage systems have been reported, but very few closo-polyhedra of any size

(16) (a) Kennedy, J. D. In *Advance in boron chemistry*; Sibert, W., Ed.; Royal Society of Chemistry: Cambridge, U.K., 1997; p 451. (b) Bould, J.; Clegg, W.; Teat, S. J.; Barton, L.; Rath, N. P.; Thornton-Pett, M.; Kennedy, J. D. Boron Chemistry at the Millennium. *Inorg. Chim. Acta* **1999**, *289*, 95 (special edition). (c) Bould, J.; Ormsby, D. L.; Yao, H.-J.; Hu, C.-H.; Sun, J.; Jin, R.-S.; Shea, S. L.; Clegg, W.; Jelinek, T.; Rath, N. P.; Thornton-Pett, M.; Greatrex, R.; Zheng, P.-J.; Barton, L.; Stibr, B.; Kennedy, J. D. In *Contemporary Boron Chemistry*; Davidson, M., Hughes, A. K., Marder, T. B., Wade, K., Eds.; Royal Society of Chemistry: Cambridge, U.K., 2000; p 171. (d) Shea, S. L.; Bould, J.; Londesborough, M. G. S.; Perera, S. D.; Franken, A.; Ormsby, D. L.; Jelinek, T.; Stibr, B.; Holub, J.; Kilner, C. A.; Thornton-Pett, M.; Kennedy, J. D. *Pure Appl. Chem.* **2003**, *75*, 1239.

(17) (a) Grimes, R. N.; Wang, F. E.; Lewin, R.; Lipscomb, W. N. *Proc. Natl. Acad. Sci. U.S.A.* **1961**, *47*, 996. (b) Grimes, R. N.; Lipscomb, W. N. *Proc. Natl. Acad. Sci. U.S.A.* **1962**, *48*, 496. (c) Plotkin, J. S.; Astheimer, R. J.; Sneddon, L. G. *J. Am. Chem. Soc.* **1979**, *101*, 4155. (d) Gaines, D. F.; Jorgenson, M. W.; Lulziek, M. A. *J. Chem. Soc., Chem. Commun.* **1979**, 380. (e) Hosmane, N. S.; Grimes, R. N. *Inorg. Chem.* **1979**, *18*, 2886. (f) Boocock, S. K.; Cheek, Y. M.; Greenwood, N. N.; Kennedy, J. D. *J. Chem. Soc., Dalton Trans.* **1981**, 1430. (g) Astheimer, R. J.; Sneddon, L. G. *Inorg. Chem.* **1983**, *22*, 1928.

(18) Bould, J.; Clegg, W.; Kennedy, J. D.; Teat, S. J. *Acta. Crystallogr., Sect. C* **2001**, *C57*, 779.

(19) Bould, J.; Londesborough, M. G. S.; Ormsby, D. L.; MacBride, J. A. H.; Wade, K.; Kilner, C. A.; Clegg, W.; Teat, S. J.; Thornton-Pett, M.; Greatrex, R.; Kennedy, J. D. *J. Organomet. Chem.* **2002**, *657*, 256.

(20) (a) Mingos, D. M. P.; Johnston, R. L. *Struct. Bonding* **1987**, *68*, 29. (b) Mingos, D. M. P.; Wales, D. J. *Introduction to Cluster Chemistry*; Prentice Hall: New York, 1990.

(21) (a) Grimes, R. N. In *Metal Interactions with Boron Clusters*; Grimes, R. N., Ed.; Plenum: New York, 1982; p 269. (b) Housecroft, C. E.; Fehlner, T. P. *Adv. Organomet. Chem.* **1982**, *21*, 57. (c) Housecroft, C. E. In *Inorganometallic Chemistry*; Fehlner, T. P., Ed.; Plenum: New York, 1992; p 73.

(22) Ghosh, S.; Fehlner, T. P.; Noll, B. C. *Chem. Commun.* **2005**, 3080.

(23) (a) Wade, K. *Inorg. Nucl. Chem. Lett.* **1972**, *8*, 559. (b) Wade, K. *Adv. Inorg. Chem. Radiochem.* **1976**, *18*, 1. (c) Wade, K. *Adv. Inorg. Chem. Radiochem.* **1976**, *18*, 67. (d) Mingo, D. M. P. *Nature (London) Phys. Sci.* **1972**, *236*, 99.

Chart 2. M_2B_6 Frameworks (M = W, Re, and Ru; B-*H*-B Hydrogens Omitted for Clarity)

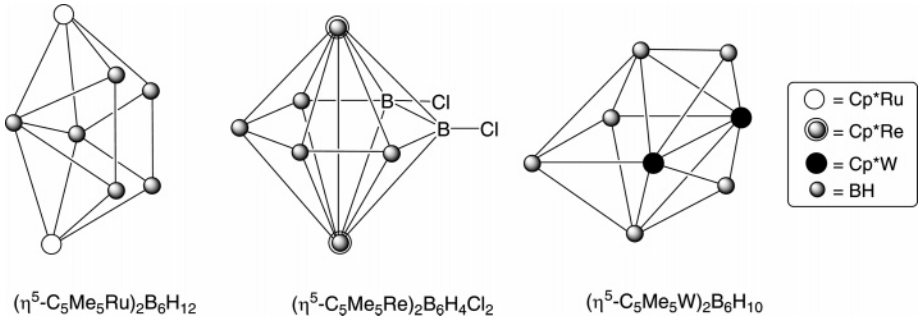

$(\eta^5\text{-}C_5Me_5Ru)_2B_6H_{12}$ $(\eta^5\text{-}C_5Me_5Re)_2B_6H_4Cl_2$ $(\eta^5\text{-}C_5Me_5W)_2B_6H_{10}$

known with bridging hydrogens. Following the reports of such species, $(CpCo)_n(BH)_{6-n}H_2$ (n = 2, 3),[24] $(\eta^5\text{-}C_5Me_5Co)_3(\mu_3\text{-}HBH)_2$[25] (which exhibit two face-bridging hydrogens), and $(\eta^5\text{-}C_5Me_5Mo)_2B_5H_9Fe(CO)_3$,[9] it appeared likely that similar types of isoelectronic compounds might exist with other transition metals. Metallaboranes **2** and **5** are the two new additions in this series. All the clusters have a skeletal electron count of 14—when regular counting rules are applied (vide infra)—and the closo-structure expected for this electron count.

Comparison of $\{Cp^*M\}_2B_6$ Clusters (M = W, Re, and Ru). We have now synthesized a set of three compounds with M_2B_6 frameworks for metals of groups 6−8. They are $(\eta^5\text{-}C_5Me_5W)_2B_6H_{10}$ (**2**), $(\eta^5\text{-}C_5Me_5Re)_2B_6H_4Cl_2$,[7] and $\{(\eta^5\text{-}C_5Me_5Ru)_2B_6H_{12}$,[4] with formal electron counts of 7, 6, and 10 sep, respectively. They are all produced under forcing conditions and reasonably represent thermodynamic minima. The molecular structures of these compounds reveal that they have different geometries despite having same number of borane fragments (Chart 2). Although not as unambiguous as the previous comparison of $(\eta^5\text{-}C_5Me_5M)_2B_4H_8$ (M = Ir, Ru, Re, Cr) for metals of group 6−9,[26−29] it still reveals the role of the metals. The structure of **2** appears to obey the electron counting rules as it is a seven-sep bicapped octahedron (a different electron-counting approach is developed below). The rhenaborane $(\eta^5\text{-}C_5Me_5Re)_2B_6H_4Cl_2$ is a closo-deltahedron and possesses a planar B_6 ring sandwiched between two Cp*Re fragments. In contrast to **2** and $(\eta^5\text{-}C_5Me_5Re)_2B_6H_4Cl_2$, $(\eta^5\text{-}C_5Me_5Ru)_2B_6H_{12}$ retains six bridging hydrogen atoms in the framework geometry. The structure is also reminiscent to 10-sep B_8H_{12} and follows the borane analogy.[30]

Although the mechanistic details of the formation of **2** and **3** from **1** are unclear, it is probable that the initial step in the generation of **3** is the formation of $(\eta^5\text{-}C_5Me_5W)_2B_5H_9$ followed by a radical generation at high temperature. The $(\eta^5\text{-}C_5Me_5W)_2B_5H_8$ radical on coupling forms **3**. The structure of **3** described above led us to attempt additional condensation of the nido tungstanoborane units, recognizing that the four W−H−B bridging protons on the open face of **4** could lead to more complex interaction between the linked clusters. However, the reaction of **3** *with* and *without* monoboron species BH_3·THF at high-temperature met either with cluster degradation or with little net reaction.

Molecular Orbital Analysis and Electron Counting Relationships. As stated above, the seven-sep bicapped octahedral architecture of cluster **2** satisfies the electron counting rules derived from the borane analogy when the classical skeletal electron counting formalism is applied. Within this framework, a BH unit contributes to the sep count with 2 electrons, a bridging hydrogen with 1 electron, and an $(\eta^5\text{-}C_5Me_5)W$ fragment with −1 electron since the three d-type so-called "t_{2g}" orbitals are assumed to generate occupied nonbonding molecular orbitals (MO) in the cluster. On the other hand, $(\eta^5\text{-}C_5Me_5Re)_2B_6H_4Cl_2$ is an electron deficient species with respect to the same formalism, since it is a six-sep [$(\eta^5\text{-}C_5Me_5)$Re: 0 electron; BH or BCl: 2 electrons] hexagonal bipyramid for which a regular count of nine sep is expected. We have shown previously that this electron deficiency is associated with the participation of some metal "t_{2g}" orbitals which play the role of sep in being significantly involved in the cluster bonding.[3] We show below that **2** can also be described as an electron deficient metallocarborane with a cluster architecture derived from that of $(\eta^5\text{-}C_5Me_5Re)_2B_6H_4Cl_2$.

Let us start with the electronic structure of $(\eta^5\text{-}C_5Me_5Re)_2B_6H_4Cl_2$ which we have simplified by the isoelectronic model $(BzMo)_2B_6H_6$ (Bz = $\eta^6\text{-}C_6H_6$) cluster in the idealized D_{6h} conformation, for the sake of working within the highest symmetry as possible. Selected DFT data corresponding to the optimized geometry of $(BzMo)_2B_6H_6$ are given in Table 1.

A simplified MO diagram is provided in Figure 4 based on the interaction of the B_6H_6 hexagon with the BzMo···MoBz dimeric fragment. The orbitals are labeled both in the D_{6h} symmetry and in the Mo···Mo pseudoaxial symmetry (i.e., σ, σ^*, π, π^*, δ, δ^*, ...). There are 18 orbitals associated with the B−B interactions in the B_6H_6 hexagon, 9 of which are bonding combinations and are susceptible to interact significantly with the metals. In the Mo···Mo pseudoaxial symmetry, the six σ (B−B) MOs span into $\sigma + \pi + \delta + \phi$. Note that the ϕ level is not doubly degenerate as expected in real axial symmetry groups, because of the lowest D_{6h} symmetry of B_6H_6. Similarly, the 3 π(B−B) levels span into $\sigma^* + \pi^*$. On the other side, each BzMo fragment possesses three hybrid-type frontier orbitals (FO) of pseudoaxial σ and π symmetry lying above the "t_{2g}" orbitals which are of pseudoaxial σ and δ symmetry. The orbital pattern for the BzMo···MoBz dimer consists of the in-phase and out-of-phase combinations of the orbitals of two noninteracting BzMo moieties as sketched in Figure 4. In a regular transition metal cluster, the t_{2g} orbitals do not participate significantly to the bonding and can be considered as nonbonding levels which are low-lying and therefore occupied.

(24) Miller, V. R.; Weiss, R.; Grimes, R. N. *J. Am. Chem. Soc.* **1977**, *99*, 5646.
(25) Deck, K. J.; Fehlner, T. P.; Rheingold, A. L. *Inorg. Chem.* **1993**, *32*, 2794.
(26) Chromium: Ho, J.; Deck, K. J.; Nishihara, Y.; Shang, M.; Fehlner, T. P. *J. Am. Chem. Soc.* **1995**, *117*, 10292.
(27) Rhenium: Ghosh, S.; Shang, M.; Fehlner, T. P. *J. Organomet. Chem.* **2000**, *614*, 92.
(28) Ruthenium: Lei, X.; Shang, M.; Fehlner, T. P. *J. Am. Chem. Soc.* **1999**, *121*, 1275.
(29) Iridium: Lei, X.; Shang, M.; Fehlner, T. P. *Organometallics* **2000**, *19*, 118.
(30) **)** (a) King, R. B. *Inorg. Chem.* **2004**, *43*, 4241. (b) Williams, R. E. In *The Borane, Carborane, Carbocation Continuum*; Casanova, J., Ed.; Wiley-Interscience: New York, 1997; p 3.

Table 1. Selected DFT Computed Data for $(BzMo)_2B_6H_6$, $(CpRe)_2B_5H_5$, $(CpRe)_2B_7H_7$, $(CpW)_2B_6H_{10}$ (2′), and $[(CpW)_2B_6H_{10}]^{2-}$

molecule symmetry	HOMO−LUMO GAP/eV	distances/Å			t_{2g} FO occupancies of the ArM···MAr (Ar = Bz, Cp) fragment (see Figure 4)			
		M−M	M−B	B−B	s	d	δ*	σ*
$(BzMo)_2B_6H_6$ D_{6h}	1.56	2.806	2.240	1.746	2.07	1.38	3.24	0.82
$(CpRe)_2B_5H_5$ C_{2v}	2.23	2.826 2.820	2.138	1.885 (×2) 1.886 1.887	1.90	0.85	3.21	1.01
$(CpRe)_2B_7H_7$ C_{2v}	2.63	2.820	2.127 2.165 2.297 2.161	1.874 1.808 1.778 1.713	1.94	1.97	2.97	1.00
$(CpW)_2B_6H_{10}$ C_{2v} (2′)	2.62	3.008	2.360 2.169 2.302	1.687 1.791 1.800	1.78	1.80	2.46	0.54
$[(BzMo)_2B_6H_6]^{2-}$ C_{2v}	1.24	2.953	2.195 2.246 2.384	1.738 1.760 1.805	0.38	2.98	3.22	1.32
$[(CpW)_2B_6H_6]^{2-}$ C_2	2.17	2.829	2.246 2.240 2.242	1.742 (×6)	1.93	1.16	3.06	0.85

We have shown previously that in the hypoelectronic dinuclear metalloboranes, three among the six t_{2g} combinations interact strongly and therefore are involved in the skeletal bonding.[3] This is the case of the σ* and δ t_{2g} combinations of the BzMo···BzMo fragment in $(BzMo)_2B_6H_6$ (Figure 4).[31] This interaction is particularly favored by the good energy match and overlap between the boron and the d-type early transition metal orbitals. Interestingly, it is still possible to identify nine sep associated with B−B and/or M−B bonding in the diagram of Figure 4. In other words, each BzMo fragment is not a donor of zero (regular counting, see above), but three skeletal electrons. Taking this statement into account, $(BzMo)_2B_6H_6$ satisfies the electron counting rules derived from the borane analogy. Thus, $(BzMo)_2B_6H_6$ is an apparent six-sep but effective nine-sep species. An important consequence of the strong involvement of the σ* t_{2g} combination in the cluster interaction is that this orbital is significantly depopulated, thus inducing direct through-cage metal−metal bonding, a characteristic of all the hypoelectronic dinuclear metalloboranes.[3] A DFT fragment molecular analysis carried out on the optimized $(BzMo)_2B_6H_6$ model is fully consistent with this qualitative description. The electron occupation of the t_{2g} σ* combination is lower than 1 in the complex, while its σ counterpart remains fully occupied (see Table 1). Similarly, the δ combinations are significantly depopulated while their δ* counterparts remain largely occupied.

Similar electronic features were found for all the hypoelectronic dinuclear metalloboranes that we have calculated, such as for example for the DFT-optimized pentagonal bipyramidal $(CpRe)_2B_5H_5$ cluster chosen as a simplified model for the apparent five-sep but effective eight-sep $(\eta^5\text{-}C_5Me_5Re)_2B_5H_4Cl_2$ compound[3] (see Table 1). Another example is the $(CpRe)_2B_7H_7$ cluster which modelizes the apparent 7-sep but effective 10-sep $(\eta^5\text{-}C_5Me_5Re)_2B_7H_6Cl$ compound (see Figure 5 and Table 1). Interestingly, $(\eta^5\text{-}C_5Me_5Re)_2B_7H_6Cl$ (or its simplified model $(CpRe)_2B_7H_7$) exhibits a skeletal geometry which is more complex than that of a simple bipyramid but which still allows the existence of through-cage metal−metal bonding (Figure 5). This shape has been related to that of a canonical nine-vertex deltahedron through diamond−square−diamond rearrangements.[3]

The title compound **2** deserves comments here. It turns out that there is a striking relationship between the isoelectronic (apparent seven-sep) clusters $(CpRe)_2B_7H_7$ and **2**. Removing the in-plane B−H fragment from $(CpRe)_2B_7H_7$ shown in Figure 5 ends up with the skeletal geometry of **2**. Thus, **2** can be seen as a nido species, related to the closo $(CpRe)_2B_7H_7$ cluster, with, as in all the hypoelectronic dinuclear metalloboranes, an additional metal−metal through-cage bond. DFT calculations on the simplified model of **2** $(CpW)_2B_6H_{10}$ (**2′**) (Figure 5) support this view, as exemplified by the large participation of the CpW t_{2g} orbitals in the bonding (Table 1). Because of the lowest symmetry of **2′** with respect to $(BzMo)_2B_6H_6$, the separation between the σ, σ*, π, π*, δ, and δ* components is not as clear as in the case of $(BzMo)_2B_6H_6$, but the trends are similar and the whole t_{2g} occupation (3.29 electrons) is particularly low. Thus, compound **2** is an apparent 7-sep but effective 10-sep species. Note that a large HOMO−LUMO gap, 2.62 eV, is computed with this electron count for the optimized cluster **2′**. The same conclusions are valid for compound **5** in which $Fe(CO)_3$ has been substituted for an isolobal BH fragment.

Another way of checking the validity of the derivation of the structure of **2** from that of the hypoelectronic metalloborane series is to formally reduce it by two electrons. Its structure should evolve toward the closo hexagonal bipyramidal geometry of $(\eta^5\text{-}C_5Me_5Re)_2B_6H_4Cl_2$. This has been checked on the apparent six-sep $[(CpW)_2B_6H_4]^{2-}$. Starting from the optimized molecular structure of the apparent seven-sep $(CpW)_2B_6H_{10}$ model (Figure 5), the geometry optimization process evolved toward the same hexagonal bipyramidal architecture as $(BzMo)_2B_6H_6$, which was found to be more stable by 0.93 eV. On the other hand, we have tested the reduction by two electrons of the hexagonal bipyramidal $(BzMo)_2B_6H_6$ model. It turns out that the expected C_{2v} structure of the apparent seven-sep

(31) (a) In the isostructural $(Cp^*Mo)_2P_6$ complex (apparent eight-sep; effective nine-sep), only one of the t_{2g} combinations (the σ* one) participates to the bonding: Tremel, W.; Hoffmann, R.; Kertesz, M. *J. Am. Chem. Soc.* **1989**, *111*, 2030. See also: Usha Rani, D.; Prasad, D. L. V. K.; Nixon, J. F.; Jemmis, E. D. *J. Comput. Chem.* **2007**, *28*, 310. (b) In a regular apparent and effective nine-sep species, the metal-ring out-of-phase combinations $\sigma^*(a_{2u})$ and $\delta(e_{2g})$ would be merely nonbonding and occupied. (c) In an electron-rich triple-decker species, the metal-ring out-of-phase combinations $\pi(e_{1u})$ would be merely nonbonding and occupied, thus increasing the electron count to 11 sep: Lauher, J. W.; Elian, M.; Summerville, R. H.; Hoffmann, R. *J. Am. Chem. Soc.* **1976**, *98*, 3219.

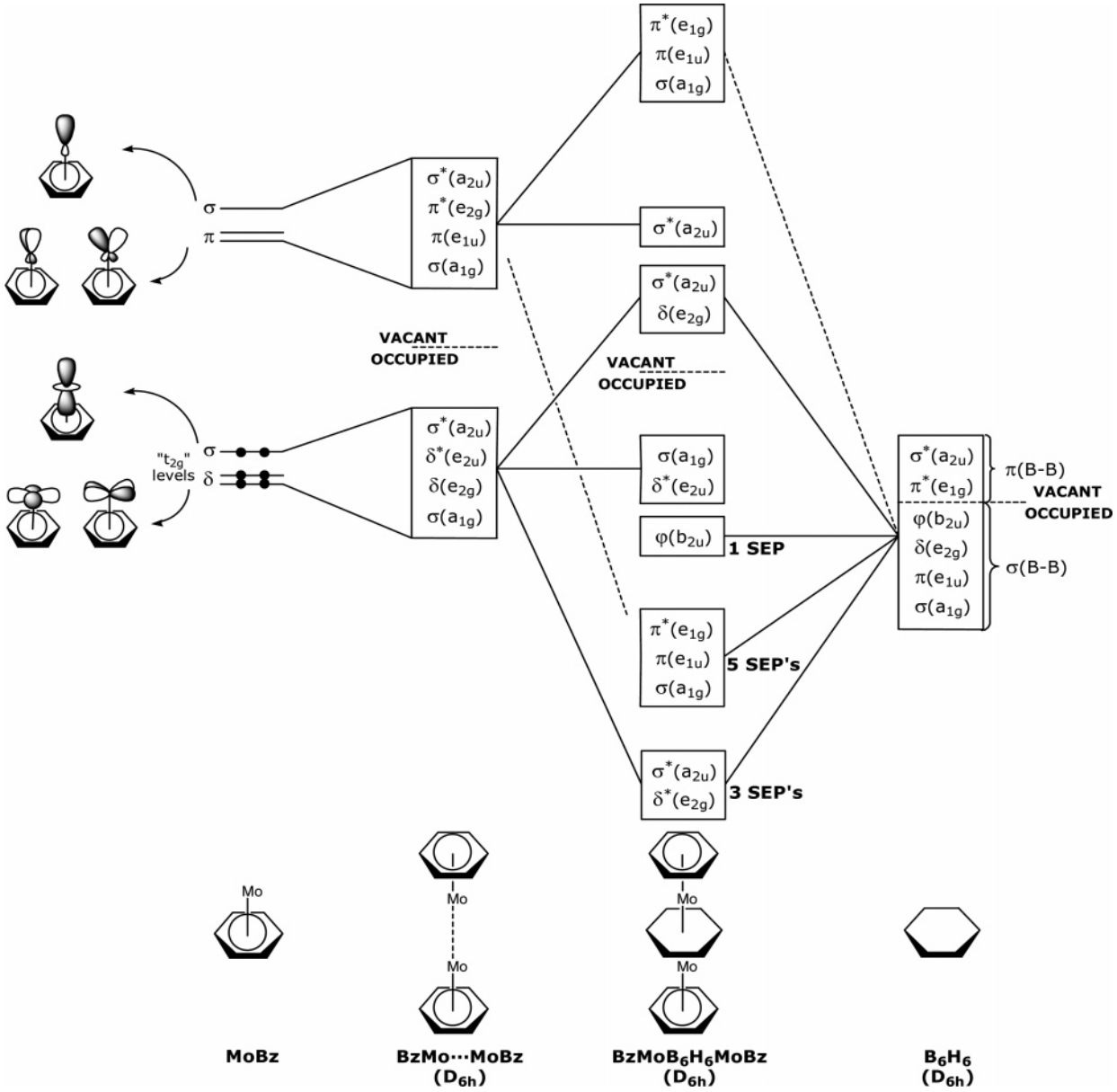

Figure 4. Schematic interaction diagram for $(BzMo)_2B_6H_6$. The MO labels σ, σ^*, π, π^*, δ, and δ^* refer to the Mo···Mo pseudoaxial symmetry.

$[(BzMo)_2B_6H_6]^{2-}$, that is, that of the isoelectronic species of **2** or **2′** (Figure 5), was found slightly less stable than that of the hexagonal bipyramidal structure which was found to be a triplet ground state. The relative instability of the $[(BzMo)_2B_6H_6]^{2-}$ C_{2v} structure is partly due to the nonlinearity of the BzMoMoBz sequence (Figure 5) which disfavors metal−metal bonding. Interestingly, the presence of four bridging hydrogens in the isostructural and isoelectronic species **2** and **2′** favors the CpWWCp linearity (compare the structures of $[(BzMo)_2B_6H_6]^{2-}$ and $(CpW)_2B_6H_{10}$ in Figure 5). Thus, the stabilization of the closo structure of **2** and **5** is partly due to the presence of bridging hydrogen atoms.

Conclusion

The geometry of a metallaborane is significantly controlled by the metal center as observed in M_2B_6 frameworks. (η^5-$C_5Me_5W)_2B_6H_{10}$, (**2**) (η^5-$C_5Me_5Re)_2B_6H_4Cl_2$, and {(η^5-$C_5Me_5Ru)_2B_6H_{12}$ have distinctly different geometries despite having same number of borane fragments. As the previous comparison of (η^5-$C_5Me_5M)_2B_4H_8$ (M = Ir, Ru, Re, Cr), this comparison clearly reveals the distinctive role of the transition metal in defining cluster structure. Further, metallaboranes with frameworks containing bridging hydrogens often exhibit nido or arachno shapes because of the spatial and electronic demands of the bridge atoms.[5,21,32] Indeed, the greater the number of bridging hydrogens, the greater the apparent tendency for open structures. The effect of bridging hydrogens has been known for many years for the boron hydrides, and, since the metal cluster fragments are frequently isolobal analogues of BH or BH_2, the effect of bridging hydrogens in metalloboranes is hardly unexpected. Cluster **2** represents an example of a closo cluster exhibiting four bridging hydrogens.

Although clusters **2** and **5** can be described as seven-sep species satisfying the capping principle and the regular electron counting rules, DFT calculations strongly suggest they are better considered as members of the family of hypoelectronic dinuclear

(32) Barton L.; Srivastava D. K. In *Comprehensive Organometallic Chemistry*, II; Abel, E., Stone, F. G. A., Wilkinson, G., Eds.; Pergamon: New York, 1995; Vol. 1.

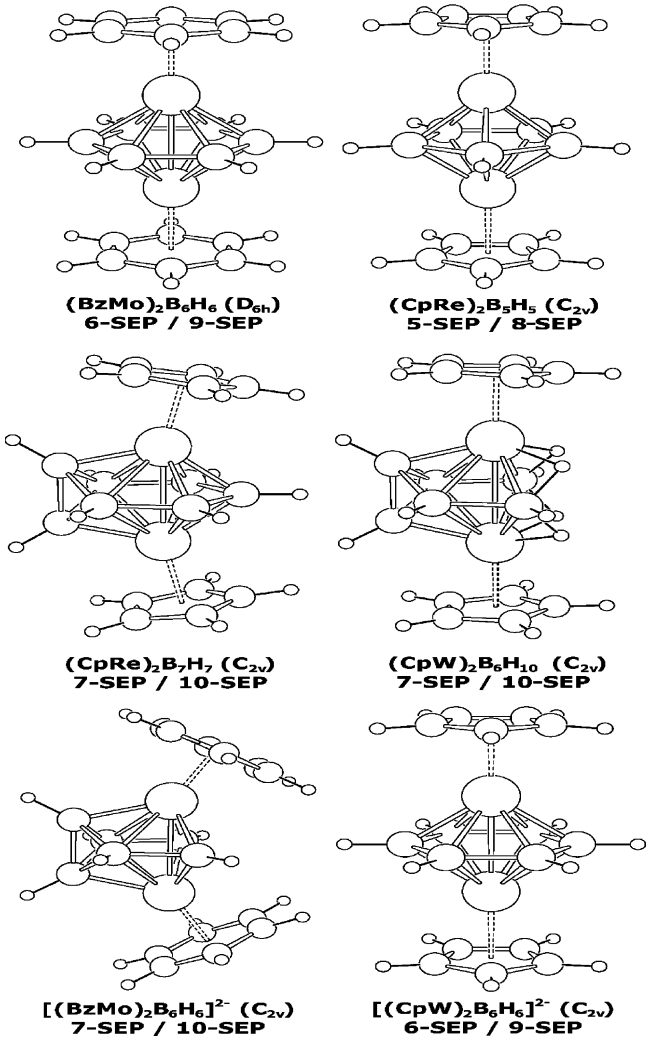

Figure 5. DFT optimized geometries of $(BzMo)_2B_6H_6$, $(CpRe)_2B_5H_5$, $(CpRe)_2B_7H_7$, $(CpW)_2B_6H_{10}$ (**2**), $[(CpW)_2B_6H_{10}]^{2-}$, and $[(BzMo)_2B_6H_6]^{2-}$. Electron counts correspond to the apparent/effective sep counts.

metalloboranes. In this type of M_2B_n clusters, three of the six t_{2g} combinations are involved in cluster bonding. One of them of σ^* (M−M) symmetry is associated with through-cage metal−metal bonding. The two others are of δ (M−M) symmetry and are used for M−B bonding. The involvement in the bonding of these δ-type frontier orbitals in addition to the σ- and π-type ones correlates with the high metal connectivities. Within this framework, **2** and **5** can be viewed as nido species with structures derived from the 9-vertex $(\eta^5\text{-}C_5Me_5Re)_2B_7H_6Cl$ closo cluster by the removal of one boron vertex. Satisfying an electron counting rule should not be construed as definitive information on true electronic structure from which chemical properties ultimately are derived.

Experimental Section

General Procedures. All the operations were conducted under an Ar/N_2 atmosphere using standard Schlenk techniques. Solvents were distilled prior to use under N_2. BH_3·THF, $LiBH_4$ in THF (Aldrich) was used as received. $\{\eta^5\text{-}C_5Me_5WH_3\}B_4H_8$ (**1**)[8] was prepared as described previously. Chromatography was carried out on 3 cm of silica gel in a 2.5 cm diameter column. Thin layer chromatography was performed on 250 mm diameter aluminum supported silica gel TLC plates. NMR spectra were recorded on a 400 MHz Bruker FT-NMR spectrometer. Residual solvent protons were used as reference (δ, ppm, benzene, 7.15), while a sealed tube containing $[Me_4N(B_3H_8)]$ in acetone-d_6 (δB, ppm, −29.7) was used as an external reference for the ^{11}B NMR. Infrared spectra were obtained on a Nicolet 205 FT-IR spectrometer. Mass spectra were obtained on a JEOL JMS-AX505HA mass spectrometer with perfluorokerosene as standard. Crystal data were collected and integrated using a Bruker Apex system, with graphite monochromated Mo Kα (λ = 0.71073 Å) radiation at 100 K. The structure was solved by heavy atom methods using SHELXS-97 and refined using SHELXL-97 (Sheldrick, G.M., University of Göttingen).

Synthesis of 2 and 3. Compound **1** (0.5 g, 1.34 mmol) in toluene (20 mL) was heated with 6-fold excess of BH_3·THF (8.02 mL, 8.04 mmol) at 95 °C for 20 h. The solvent was evaporated in vacuo; residue was extracted into hexane and passed through a mixture of Celite and silica gel. After removal of solvent from filtrate, the residue was subjected to chromatographic workup using silica gel TLC plates. Elution with hexane/CH_2Cl_2 (70:30 v/v) yielded light yellow $(\eta^5\text{-}C_5Me_5W)_2B_6H_{10}$ (**2**) (0.11 g, 12%) and orange-yellow $\{(\eta^5\text{-}C_5Me_5W)_2B_5H_8\}_2$ (**3**) (0.09 g, 5%). X-ray quality crystals were grown by slow diffusion of a hexane/CH_2Cl_2 (9.5:0.5 v/v) solution of **2** and **3** at 4 °C. **2**: MS (FAB) P^+(max) 713 (isotopic pattern for 2W and 6B atoms), $^{12}C_{20}{}^1H_{40}{}^{11}B_6{}^{183}W_2$ calcd, 714.2707; obsd, 714.2679. ^{11}B NMR (C_6D_6, 22 °C): δ 83.9 (d, J_{B-H} = 144 Hz, 2B), δ 47.9 (s, J_{B-H} = 120 Hz, 2B), δ -12.7 (d, J_{B-H} = 131 Hz, 2B). $^1H\{^{11}B\}$ NMR (C_6D_6, 22 °C): δ 9.74 (partially collapsed quartet (pcq), 2 BH_t), δ 6.96 (pcq, 2 BH_t), δ 1.17 (pcq, 2 BH_t), δ 1.96 (s, 30H, Cp*), δ −15.79 (s, br, 4W-H−B). IR (hexane, cm^{-1}): 2504w, 2446w ν(B−H_t). **3**: MS (FAB) P^+(max) 1399 (isotopic pattern for 4W and 10B atoms). ^{11}B NMR (C_6D_6, 22 °C): δ 50.6 (br, 1B), δ 48.3 (d, J_{B-H} = 131 Hz, 2B), δ 40.6 (br, 1B), δ 26.1 (br, 1B). $^1H\{^{11}B\}$ NMR (C_6D_6, 22 °C): δ 6.29 (pcq, 2 BH_t), δ 6.12 (pcq, 1 BH_t), δ 3.72 (pcq, 1 BH_t), δ 2.23 (s, 30H, Cp*), δ 2.13 (s, 30H, Cp*), δ −5.74 (s, br, 1W−H−B), δ-6.16 (s, br, 1W−H−B), δ-8.60 (s, br, 1W−H−B), δ-8.90 (s, br, 1W−H−B). IR (hexane, cm^{-1}): 2504w, 2438w ν(B−H_t).

Preparation of 5. Compound **4** (0.3 g, 0.42 mmol) in hexane (25 mL) was heated with 3-fold excess of $Fe_2(CO)_9$ (0.46 g, 1.28 mmol) at 55 °C for 72 h. The solvent was evaporated in vacuo, and the residue was extracted into hexane and passed through celite. The green-color filtrate was concentrated and kept at −40 °C to remove $Fe_3(CO)_{12}$. After removal of $Fe_3(CO)_{12}$ the mother liquor was subjected to chromatographic workup using silica gel TLC plates. Elution with hexane/CH_2Cl_2 (85:15 v/v) yielded $(\eta^5\text{-}C_5Me_5W)_2B_5H_9Fe(CO)_3$ (**5**) (0.16 g, 46%). X-ray quality crystals were grown by slow diffusion of a hexane solution of **5** at 4 °C. **5**: MS (FAB) P^+(max) 841 (isotopic pattern for 2W, 1Fe, and 5B atoms); $^{12}C_{23}{}^1H_{39}{}^{183}W_2{}^{16}O_3{}^{55}Fe_1{}^{11}B_5$ calcd, 842.1733; obsd, 842.1697. ^{11}B NMR (C_6D_6, 22 °C): δ84.2 (d, J_{B-H} = 120 Hz, 2B), δ46.2 (br, 1B), δ39.1 (br, 1B), δ-6.6 (d, J_{B-H} = 139 Hz, 1B). $^1H\{^{11}B\}$ NMR (C_6D_6, 22 °C): δ8.65 (pcq, 2 BH_t), 6.51 (pcq, 1 BH_t), δ4.41 (pcq, 1 BH_t), δ0.94 (pcq, 1 BH_t), δ1.88 (s, 30H, Cp*), δ-15.33 (s, br, 2W−H−B), δ-16.92 (s, br, 2W−H−B). IR (hexane, cm^{-1}): 2498w, 2420w ν(B−H_t), 2014s, 1965 m, 1948 m ν(C−O).

X-ray Structure Determination. Crystal Data for 2. Formula, $C_{20}H_{40}B_6W_2$; crystal system, monoclinic; space group, $P2(1)/n$. Unit cell dimensions: a = 10.9284(2) Å, α = 90°, b = 16.2110(3) Å, β = 111.2280(10)°, c = 14.5162(3) Å, γ = 90°, Z = 4. Density (calcd) = 1.976 Mg/m^3. Final R indices [$I > 2\sigma(I)$]: $R1$ = 0.0179, w$R2$ = 0.0431. Index ranges = $-15 \le h \le 15$, $-14 \le k \le 22$, $-20 \le l \le 20$. Crystal size = 0.17 × 0.16 × 0.12 mm^3. Reflections collected, 31703; independent reflections, 6986, [R(int) = 0.0299]; observed reflections ($I > 2\sigma(I)$), 6317; GOF on F^2 = 1.047.

Crystal Data for 3. Formula, $C_{46}H_{90}B_{10}W_4$; crystal system, monoclinic; space group, $C2/c$. Unit cell dimensions: a = 26.1177(15) Å, α = 90°, b = 11.8095(7) Å, β = 116.866(2)°, c = 19.0493(11) Å, γ = 90°, Z = 4. Final R indices [$I > 2\sigma(I)$]: $R1$ = 0.0526, w$R2$ = 0.1336. Index ranges = $-34 \le h \le 31$, $0 \le k \le 15$, $0 \le l \le 25$. θ range for data collection = 1.75−28.30°. Crystal size =

0.26 × 0.21 × 0.13 mm^3. Density (calcd) = 1.884 Mg/m^3. Reflections collected, 55128; independent reflections, 8661 [*R*(int) = 0.0835]; observed reflections ($I > 2\sigma(I)$), 6744; GOF on F^2 = 1.049.

Crystal data for 5. Formula, $C_{23}H_{39}B_5FeO_3W_2$; crystal system, orthorhombic; space group, *Fdd*2. Unit cell dimensions: a = 24.4894(19) Å, b = 24.813(2) Å, c = 17.8206(15) Å, $\alpha = \beta = \gamma = 90°$, Z = 16. Final R indices [$I > 2\sigma(I)$]: $R1 = 0.0483$, $wR2 = 0.1221$. Index ranges = $-36 \le h \le 37$, $-38 \le k \le 30$, $-27 \le l \le 21$. θ range for data collection = 1.63−33.14°. Crystal size = 0.34 × 0.14 × 0.14 mm^3. Density (calcd) = 2.064 Mg/m^3. Reflections collected, 32631; independent reflections, 8891 [*R*(int) = 0.0434]; observed reflections ($I > 2\sigma(I)$), 7887; GOF on F^2 = 1.023.

Computational Details. DFT[33] calculations were carried out using the ADF package.[34] The VWN parametrization[35] was used to treat electron correlation within local density approximation plus the nonlocal BP86 corrections.[36,37] The numerical integration procedure applied for the calculations was developed by te Velde.[33d] The standard ADF TZP atomic basis sets was used for all the atoms. The frozen core approximation was used to treat core electrons,[33d] at the following level: C, B, 1s; Mo, 3d; W, Re, 4d. Full geometry optimizations were carried out on each complex using the analytical gradient method implemented by Verluis and Ziegler.[38] Spin-unrestricted calculations were performed for the open-shell systems. Fragment interaction analysis was done using the method proposed by Ziegler.[39] Relativistic corrections were added by the use of the ZORA (zeroth-order regular approximation) scalar Hamiltonian for rhenium and tungsten compounds.[40]

Acknowledgment. S.K.B. thanks the University Grants Commission, India, for a Junior Research Fellowship. Generous support of the National Science Foundation under Grant CHE 0304008 is gratefully acknowledged. These studies were also facilitated by travel grants (NSF INT 02-31792, USA and the Centre National de la Recherche Scientifique (CNRS 03N92/0123), France). Calculations were carried out at the French national computing centers IDRIS (Orsay) and CINES (Montpellier).

Supporting Information Available: CIF files for **2**, **3**, and **5** as well as Cartesian coordinate of the DFT optimized structures. This material is available free of charge via the Internet at http://pubs.acs.org.

OM700565F

(33) (a) Baerends, E. J.; Ellis, D. E.; Ros, P. *Chem. Phys.* **1973**, *2*, 41. (b) Baerends, E. J.; Ross, P. *Int. J. Quantum Chem.* **1978**, *S12*, 169. (c) Boerrigter, P. M.; te Velde, G.; Baerends, E. J. *Int. J. Quantum Chem.* **1988**, *33*, 87. (d) te Velde, G.; Baerends, E. J. *J. Comput. Phys.* **1992**, *99*, 84.

(34) *Amsterdam Density Functional (ADF) program*, version ADF2005.01; SCM, Vrije Universiteit: Amsterdam, Netherlands, 2005.

(35) Vosko, S. D.; Wilk, L.; Nusair, M. *Can. J. Chem.* **1990**, *58*, 1200.

(36) (a) Becke, A. D. *J. Chem. Phys.* **1986**, *84*, 4524. (b) Becke, A. D. *Phys. Rev. A* **1988**, *38*, 2098.

(37) (a) Perdew, J. P. *Phys. Rev. B* **1986**, *33*, 8882. (b) Perdew, J. P. *Phys. Rev. A* **1986**, *34*, 7406.

(38) Verluis, L.; Ziegler, T. *J. Chem. Phys.* **1988**, *88*, 322.

(39) te Velde, G.; Bickelhaupt, F. M.; Fonseca Guerra, C.; van Gisbergen, S. J. A.; Baerends, E. J.; Snijders, J. G.; Ziegler, T. J. T. *J. Comput. Chem.* **2001**, *22*, 931.

(40) (a) van Lenthe, E.; Baerends, E. J.; Snijders, J. G. *J. Chem. Phys.* **1993**, *99*, 4597. (b) van Lenthe, E.; Baerends, E. J.; Snijders, J. G. *J. Chem. Phys.* **1994**, *101*, 9783. (c) van Lenthe, E.; van Leeuwen, R.; Baerends, E. J. *Int. J. Quantum Chem.* **1996**, *57*, 281.